Bioorganic & Medicinal Chemistry Letters xxx (2014) xxx–xxx

Contents lists available at ScienceDirect

Bioorganic & Medicinal Chemistry Letters

journal homepage: www.elsevier.com/locate/bmcl

Synthesis, biological evaluation and molecular modeling study of 2-(1,3,4-thiadiazolyl-thio and 4-methyl-thiazolyl-thio)-quinazolin-4-ones as a new class of DHFR inhibitors

Sarah T. Al-Rashood [a], Ghada S. Hassan [b,*], Shahenda M. El-Messery [c], Mahmoud N. Nagi [d], El-Sayed E. Habib [e], Fatmah A. M. Al-Omary [a], Hussein I. El-Subbagh [b,*]

[a] Department of Pharmaceutical Chemistry, College of Pharmacy, King Saud University, PO Box 2457, Riyadh 11451, Saudi Arabia
[b] Department of Medicinal Chemistry, Faculty of Pharmacy, Mansoura University, PO Box 35516, Mansoura, Egypt
[c] Department of Pharmaceutical Organic Chemistry, Faculty of Pharmacy, Mansoura University, PO Box 35516, Mansoura, Egypt
[d] Department of Pharmacology, College of Pharmacy, King Saud University, Riyadh 11451, Saudi Arabia
[e] Department of Pharmaceutics and Pharmaceutical Technology (Microbiology), College of Pharmacy, Taibah University, Almadinah Almunawwarah 344, Saudi Arabia

ARTICLE INFO

Article history:
Received 2 May 2014
Accepted 28 July 2014
Available online xxxx

Keywords:
Synthesis
Quinazolin-4-ones
DHFR inhibition
Antimicrobial testing
Antitumor screening
Molecular modeling study

ABSTRACT

A new series of 2-(1,3,4-thiadiazolyl- or 4-methyl-thiazolyl)thio-6-substituted-quinazolin-4-one analogs was designed, synthesized, and evaluated for their in vitro DHFR inhibition, antimicrobial, and antitumor activities. Compounds **29**, **34**, and **39** proved to be the most active DHFR inhibitors with IC_{50} values range of 0.1–0.6 μM. Compounds **28**, **31** and **33** showed remarkable broad-spectrum antimicrobial activity comparable to the known antibiotic Gentamicin. Compounds **26**, **33**, **39**, **43**, **44**, **50**, **55** and **63** showed broad spectrum antitumor activity with GI values range of 10.1–100%. Molecular modeling study concluded that recognition with key amino acid Glu30, Phe31 and Phe34 is essential for binding. ADMET properties prediction of the active compounds suggested that compounds **29** and **34** could be orally absorbed with diminished toxicity.

Dihydrofolate reductase (DHFR) catalyzes the reduction of dihydro folate to tetrahydrofolate which couples with thymidylate synthase in the reductive methylation of deoxyuridine to deoxythymidine. The inhibition of DHFR activity leads to cellular deficiency of tetrahydrofolate cofactors that result in cell death.[1,2] DHFR inhibition has long been identified as an important target for the development of chemotherapeutic agents against bacterial and parasitic infections as well as cancer.[3] DHFR inhibitors are broadly classified as either classical or non-classical antifolates. Literature citations revealed numerous compounds which categorized under the non-classical DHFR inhibitors such as: Trimethoprim (TMP, **A**), trimetrexate (TMQ, **B**) and piritrexim (PTX, **C**), beside others belong to the quinazoline heterocycle,[4–12] (Chart 1).

Recently, a new series of 2,3,6-substituted-quinazolin-4-ones was designed, synthesized, and evaluated for their in vitro DHFR inhibition in our laboratories.[13–17] The type of 2-, 3- or 6-substituent on the studied quinazolines manipulated and affected the magnitude of the DHFR inhibition activity. This study allowed the allocation of compounds **D**–**I** as active DHFR inhibitors with IC_{50} values around 0.4 μM. (Chart 1). Compounds **D** and **F** characterized by bearing 2-thioallylic hydrophobic π-system,[14] while compounds **G**–**I** characterized by bearing 2-thiazolyl-thio π-system.[15] Molecular modeling studies of this class of compounds revealed the importance of the main pharmacophoric groups (the 4-carbonyl fragment, the basic nitrogen atom at N-1, and the hydrophobic π-system regions) as well as of their relative spatial distances. The substitution pattern and spatial considerations of the π-systems in regard to the quinazoline nucleus proved to be critical for DHFR inhibition.[13–17]

In continuation to our previous efforts,[13–30] a new series of quinazolin-4-one analogs was designed bearing 2-(1,3,4-thiadiazolyl- or 4-methyl-thiazolyl-)thio-functions as hydrophobic π-system regions replacing the 2-thioalkyl or 2-thioallyl function of the lead compounds **D**–**F**; and as isosters of the prototypes **G**–**I** to explore the scope and limitations of this new class of DHFR inhibitors. In addition, 6-chloro, 6-methyl, or 6,7-dimethoxy functions, representing electron donating and electron withdrawing substituents; a phenyl or benzyl group at position 3- were introduced to the quinazolin-4-one nucleus in resemblance to the leads **D**–**I**. Most of the functions designed to be accommodated on the quinazoline

* Corresponding authors. Tel.: +20 50 2247800; fax: +20 50 2247900.
E-mail addresses: ghadak25@yahoo.com (G.S. Hassan), subbagh@yahoo.com (H.I. El-Subbagh).

http://dx.doi.org/10.1016/j.bmcl.2014.07.070
0960-894X/

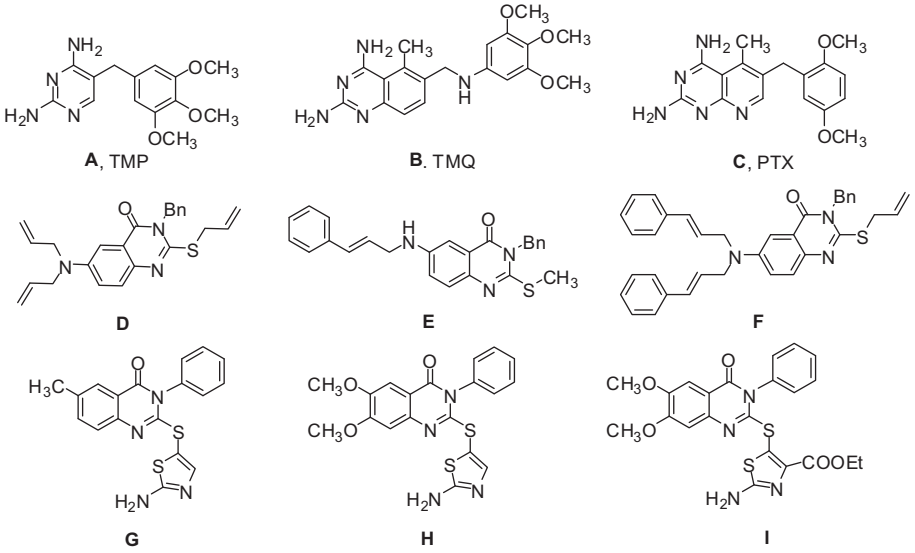

Chart 1. Structures of some literature antifolate lead compounds.

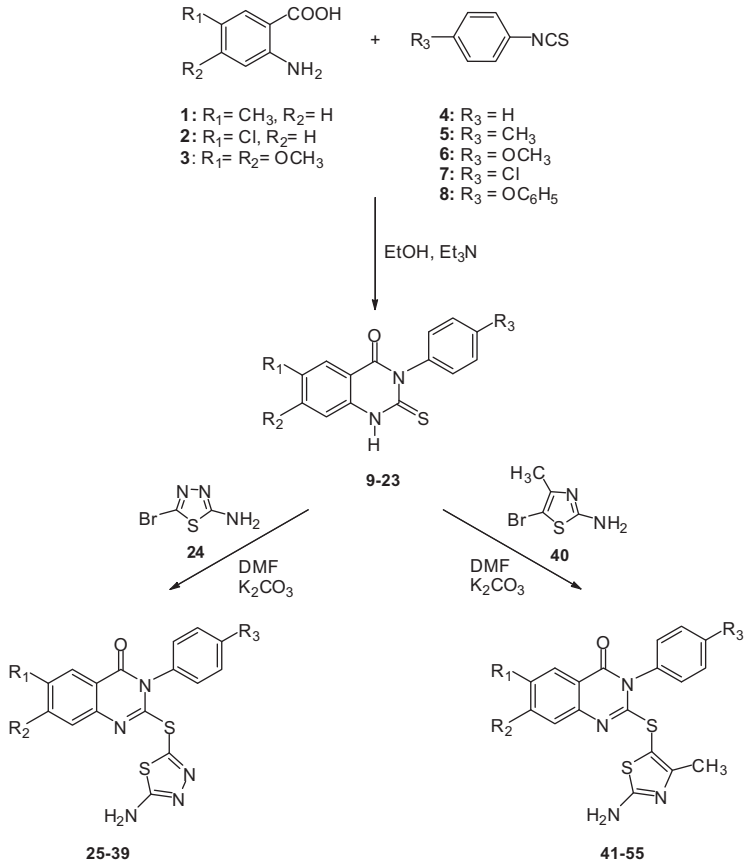

Scheme 1. Synthesis of the target compounds **25**–**39** and **41**–**55**.

ring such as thioether, heteroaryl groups are known to contribute to DHFR inhibition activity.[31,32] The aim of this study is to locate novel synthetic lead compound(s), and their in vitro testing as DHFR inhibitor(s). Compounds possessing DHFR inhibition activity are candidates for treating cancer and bacterial infections. Accordingly, the obtained derivatives were tested for their in vitro antimicrobial activity against a panel of standard strains of Gram-positive and Gram-negative bacteria, and screened for their in vitro antitumor activity using the NCI's disease-oriented human cell lines assay.[33–36]

The synthetic strategy to obtain the target compounds is depicted in Schemes 1 and 2. The starting materials 6-methyl-3-substituted-2-thioxo-2,3-dihydro-quinazolin-4(1*H*)-ones (**9**–**13**), 6-chloro-3-sub-stituted-2-thioxo-2,3-dihydro-quinazolin-4(1*H*)-ones (**14**–**18**), 6,7-dimethoxy-3-substituted-2-thioxo-2,3-dihydro-quinazolin-4(1*H*)-ones (**19**–**23**) and 3-benzyl-6-substituted or

6,7-disubstituted-2-thioxo-2,3-dihydro-quinazolin-4(1*H*)-ones (**57**–**59**) were prepared adopting reported procedures.[29,30] The 2-thioxo-function of the starting materials **9**–**23** was then alkylated using either 2-amino-5-bromo-1,3,4-thiadiazole (**24**), or 2-amino-5-bromo-4-methylthiazole (**40**) in dimethylformamide (DMF) in presence of potassium carbonate to afford 2-(5-amino-1,3,4-thiadiazol-2-yl-thio)-3-(4-substituted-phenyl)-6-substituted or 6,7-disub-stituted-quinazolin-4(3*H*)-ones (**25**–**39**) and 2-(2-amino-4-methylthiazol-5-yl-thio)-3-(4-substituted-phenyl)-6-substituted or 6,7-disubstituted-quinazolin-4(3*H*)-ones (**41**–**55**) respectively, Scheme 1. Similarly, the 2-thioxo-function of the starting materials **57**–**59** was reacted with **24** or **40** under the same conditions to afford 2-(5-amino-1,3,4-thiadiazol-2-yl-thio)-3-benzyl-6-substituted or 6,7-disubstituted-quinazolin-4(3*H*)-ones (**60**–**62**) and 2-(2-amino-4-methylthiazol-5-ylthio)-3-benzyl-6-substituted or 6,7-disubstituted-quinazolin-4(3*H*)-ones (**63**–**65**) respectively, Scheme 2. Structure elucidation of the synthesized intermediates and final products was attained by the aid of elementary analyses, ^{1}H & ^{13}C NMR spectroscopy, and mass spectrometry. The characteristic 2-amino function attached to the thiadiazole nucleus in **25**–**39** and **60**–**62** appeared as exchangeable singlet in their respective ^{1}H NMR spectra, while the 3H singlet peak at δ 2.5 δ ppm indicates the presence of the 4-methyl amino-thiazole moiety in compounds **41**–**55** and **63**–**65**. The ^{13}C-NMR spectra of the synthesized compounds were in agreement with the proposed structures. For instance, compound **27** showed 18 absorption carbon peaks, the carbonyl and imine carbons of the quinazolinone ring resonated at δ 175.9 and 160.2 ppm, respectively, while different aromatic carbons resonated at δ 125.8–159.2 ppm (Table 1).

The synthesized compounds (**25**–**39**, **41**–**55**, and **60**–**65**) were evaluated as inhibitors of bovine liver DHFR using reported procedure.[37] Results were reported as IC_{50} values (Tables 2). Compounds **28**, **29**, **32**–**34**, **36**, **39**, **50** and **53** proved to be the most active DHFR inhibitors with IC_{50} values range of 0.1–1.0 μM, while compounds **27**, **41**, **45**–**47**, **54**, **60**, **63**, **64** were considered of moderate activity with IC_{50} range of 1.0–5.0 μM, the rest of the tested compounds were considered to be inactive with IC_{50} > 5 μM. Methotrexate (IC_{50} 0.008 μM) was used as a positive control.

The synthesized compounds (**25**–**39**, **41**–**55**, and **60**–**65**) were tested for their in vitro antimicrobial activity against a panel of standard strains of the Gram-positive bacteria (*Staphylococcus aureus* and *Bacillus subtilis*), the Gram-negative bacteria (*Escherichia coli* and *Pseudomonas aeuroginosa*), and the yeast-like pathogenic fungus *Candida albicans*. The primary screen was carried out using the agar disc-diffusion method using Müller-Hinton agar medium.[38,39] The broad spectrum antibiotic Gentamicin (100 μg/disc), and the DHFR inhibitor Sulphacetamide (100 μg/disc) were used as positive controls. The obtained results revealed that the tested compounds expressed varying degrees of activity against the tested microorganisms (Table 2). Strong activity (>15 mm inhibition zone) against the Gram-positive bacteria was observed for compounds **28**, **31**, **33**, **45**, **47** and **63**–**65** against *S. aureus* and *B. subtilis*. Compounds **28**, **45** and **65** showed activity comparable to the used positive controls. In case of Gram-negative bacteria, strong activity was observed for compounds **28**, **31** and **33** against *E. coli*. Compounds **28**, **31** and **33** showed a remarkable broad-spectrum activity against both Gram-positive and Gram-negative bacteria. Compounds **45**, **47** and **63**–**65** appeared to be selective and active against gram positive bacteria. The minimal inhibitory concentrations (MICs) for the most

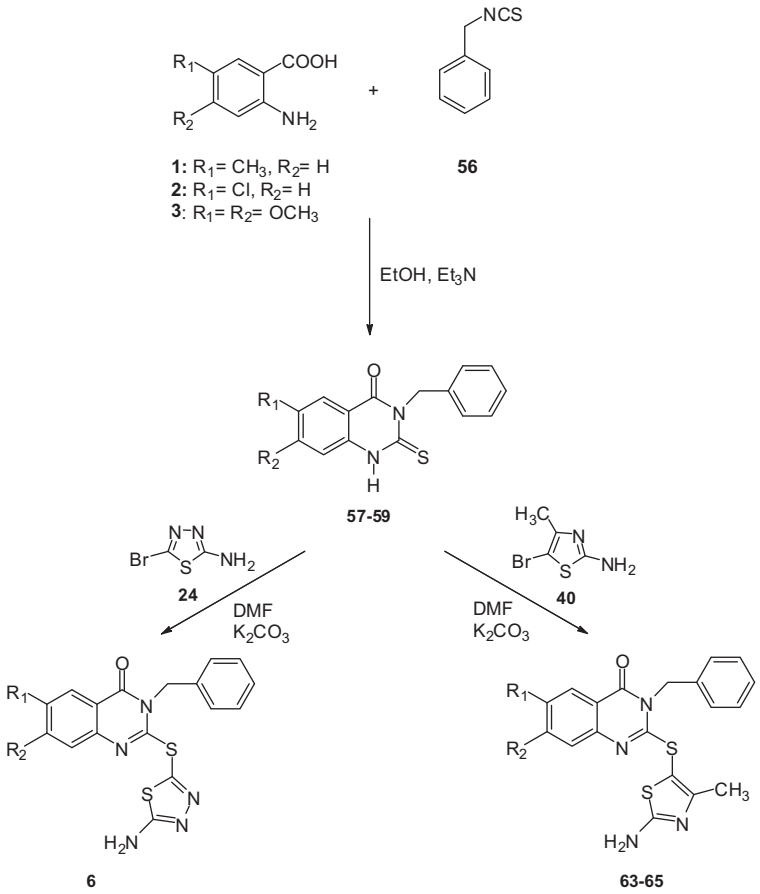

Scheme 2. Synthesis of the target compounds **60**–**62** and **63**–**65**.

Table 1
Physicochemical properties of the synthesized compounds **25**–**39**, **41**–**55**, and **60**–**65**

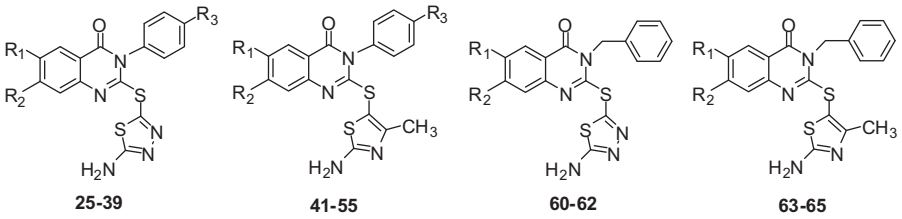

Compd	R_1	R_2	R_3	Yield %	Mp °C	Molecular formulae[a]
25	CH_3	H	H	54	153–5	$C_{17}H_{13}N_5OS_2$
26	CH_3	H	CH_3	66	173–6	$C_{18}H_{15}N_5OS_2$
27	CH_3	H	OCH_3	52	151–3	$C_{18}H_{15}N_5O_2S_2$
28	CH_3	H	Cl	60	133–5	$C_{17}H_{12}ClN_5OS_2$
29	CH_3	H	OC_6H_5	74	192–4	$C_{23}H_{17}N_5O_2S_2$
30	Cl	H	H	44	174–6	$C_{16}H_{10}ClN_5OS_2$
31	Cl	H	CH_3	59	126–8	$C_{17}H_{12}ClN_5OS_2$
32	Cl	H	OCH_3	49	162–4	$C_{17}H_{12}ClN_5O_2S_2$
33	Cl	H	Cl	75	135–7	$C_{16}H_9Cl_2N_5OS_2$
34	Cl	H	OC_6H_5	79	182–4	$C_{22}H_{14}ClN_5O_2S_2$
35	OCH_3	OCH_3	H	45	166–8	$C_{18}H_{15}N_5O_3S_2$
36	OCH_3	OCH_3	CH_3	55	156–8	$C_{19}H_{17}N_5O_3S_2$
37	OCH_3	OCH_3	OCH_3	68	110–3	$C_{19}H_{17}N_5O_4S_2$
38	OCH_3	OCH_3	Cl	51	121–4	$C_{18}H_{14}ClN_5O_3S_2$
39	OCH_3	OCH_3	OC_6H_5	70	133–5	$C_{24}H_{19}N_5O_4S_2$
41	CH_3	H	H	62	167–9	$C_{19}H_{16}N_4OS_2$
42	CH_3	H	CH_3	54	143–5	$C_{20}H_{18}N_4OS_2$
43	CH_3	H	OCH_3	59	182–4	$C_{20}H_{18}N_4O_2S_2$
44	CH_3	H	Cl	50	166–8	$C_{19}H_{15}ClN_4OS_2$
45	CH_3	H	OC_6H_5	55	132–4	$C_{25}H_{20}N_4O_2S_2$
46	Cl	H	H	64	160–2	$C_{18}H_{13}ClN_4OS_2$
47	Cl	H	CH_3	43	154–6	$C_{19}H_{15}ClN_4OS_2$
48	Cl	H	OCH_3	59	133–5	$C_{19}H_{15}ClN_4O_2S_2$
49	Cl	H	Cl	58	188–90	$C_{18}H_{12}Cl_2N_4OS_2$
50	Cl	H	OC_6H_5	69	196–8	$C_{24}H_{17}ClN_4O_2S_2$
51	OCH_3	OCH_3	H	58	154–7	$C_{20}H_{18}N_4O_3S_2$
52	OCH_3	OCH_3	CH_3	55	122–4	$C_{21}H_{20}N_4O_3S_2$
53	OCH_3	OCH_3	OCH_3	49	135–7	$C_{21}H_{20}N_4O_4S_2$
54	OCH_3	OCH_3	Cl	62	158–60	$C_{20}H_{17}ClN_4O_3S_2$
55	OCH_3	OCH_3	OC_6H_5	68	194–6	$C_{26}H_{22}N_4O_4S_2$
60	CH_3	H	—	41	160–2	$C_{18}H_{15}N_5OS_2$
61	Cl	H	—	53	144–9	$C_{17}H_{12}ClN_5OS_2$
62	OCH_3	OCH_3	—	39	141–3	$C_{19}H_{17}N_5O_3S_2$
63	CH_3	H	—	68	175–7	$C_{20}H_{18}N_4OS_2$
64	Cl	H	—	72	122–4	$C_{19}H_{15}ClN_4OS_2$
65	OCH_3	OCH_3	—	56	162–4	$C_{21}H_{20}N_4O_3S_2$

[a] Compounds analyzed for C,H,N,; results were within ± 0.4 % of the theoretical values for the given formulae.

active compounds were carried out using the micro-dilution susceptibility method. Comparing the potency of the active antibacterial compounds and their DHFR inhibition revealed that compounds **28** and **33** might exert their activity through DHFR inhibition.

The synthesized compounds (**25**–**39**, **41**–**55**, and **60**–**65**) were subjected to the National Cancer Institute (NCI) in vitro disease-oriented human cells screening panel assay for in vitro antitumor activity. A single dose (10 μM) of the test compounds were used in the full NCI 60 cell lines panel assay which includes nine tumor subpanels namely; Leukemia, Non-small cell lung, Colon, CNS, Melanoma, Ovarian, Renal, Prostate, and Breast cancer cells.[33–36] The data reported as mean-graph of the percent growth of the treated cells, and presented as percentage growth inhibition (GI %) caused by the test compounds. Compounds **26**, **33**, **38**, **39**, **43**, **44**, **50**, **55** and **63** showed broad spectrum potency toward several tumor cell lines with GI values range of 10.1–100%. Concerning activity toward individual cell lines, leukemia CCRF-CEM and HL-60(TB) cell lines showed sensitivity toward compound **50** with GI values of 58.5% and 40.6%, respectively; MOLT-4 cell line toward **50** and **55** with GI values of 55.7% and 46.1%, respectively; RPMI-8226 cell line toward **39** with GI value of 43.7%, also SR cell line toward compound **39** and **44** with GI values of 57.3% and 49.2%, respectively; while compounds **50** and **55** proved lethal to this particular cell line. Non-small cell lung cancer HOP-92 proved sensitive toward compounds **32**, **33**, **38**, **43**, **44** and **63** with GI values of 42.1%, 53.7%, 40.9%, 42.3%, 43.3% and 50.2%, respectively. Compound **50** showed GI values of 66.7%, 44.6% and 44.1% toward HCT-116, HCT-15, and HT29, respectively; while compound **55** showed GI value of 52.7% against HCT-116 Colon cancer. OVCAR-4 ovarian cancer cell line proved sensitive toward compounds **50** and **55** with GI values of 59.1% and 49.3%, respectively. Regarding renal cancer cell lines, compound **44** showed GI values of 53.0% and 46.0% against A498 and UO-31, respectively; while compound **50** showed GI value of 60.2% against A498. Finally, concerning prostate cancer cell lines, compound **50** showed GI values of 51.1% against PC-3 cell line (Tables 3 and 4). Comparing the potency of the active antitumor compounds and their DHFR inhibition revealed that compounds **33**, **39** and **50** might exert their antitumor activity through DHFR inhibition.

Please cite this article in press as: Al-Rashood, S. T.; et al. *Bioorg. Med. Chem. Lett.* (2014), http://dx.doi.org/10.1016/j.bmcl.2014.07.070

Table 2
DHFR inhibition (IC_{50}, μM), and antimicrobial activity results of compounds **25**–**39**, **41**–**55**, and **60**–**65**

Compd	DHFR inhibition	Inhibition Zone (mm)				
		S. aureus	*B. subtilis*	*E. coli*	*P. aeuroginosa*	*C albicans*
25	7	–	–	–	–	–
26	8	–	–	–	–	–
27	3	–	–	–	–	–
28	0.7	24 (2.0)	26 (2.0)	18 (2.0)	12	–
29	0.1	–	–	–	–	–
30	6	–	–	–	–	–
31	8	18 (8.0)	20 (4.0)	18 (4.0)	14	10
32	0.8	–	–	–	–	–
33	1	18 (8.0)	20 (4.0)	16 (8.0)	12	–
34	0.4	–	–	–	–	–
35	10	–	–	–	–	–
36	1	14	15	–	–	–
37	7	–	–	–	–	–
38	6	–	–	–	–	–
39	0.6	–	–	–	–	–
41	5	–	–	–	–	–
42	7	–	–	–	–	–
43	7	–	–	–	–	–
44	7	–	–	–	–	–
45	2	26 (2.0)	22 (2.0)	14	–	–
46	5	–	–	–	–	–
47	5	18 (8.0)	16 (8.0)	–	–	–
48	8	–	–	–	–	–
49	8	–	–	–	–	–
50	1	–	–	–	–	–
51	7	–	–	–	–	–
52	8	–	–	–	–	–
53	1	–	–	–	–	–
54	2	18	14	–	–	–
55	6	–	–	–	–	–
60	2	–	–	–	–	–
61	8	–	–	12	–	–
62	6	–	14	–	–	–
63	5	18 (4.0)	21 (2.0)	–	–	12
64	5	18 (4.0)	19 (4.0)	12	–	–
65	6	20 (4.0)	24 (2.0)	–	–	–
Gentamicin	–	27 (2.0)	25 (2.0)	18 (2.0)	21 (0.5)	19 (1.0)
Sulphacetamide	–	20 (2.0)	22 (2.0)	18 (2.0)	28 (1.0)	25 (2.0)

(–) Not active (8 mm), Weak activity (8–12 mm), Moderate activity (12–15 mm), Strong activity (>15 mm). Solvent: DMSO (8 mm). MICs showed in parentheses.

In the present investigation, the type of 2-, 3- or 6-substituent on the studied quinazolines manipulated the DHFR inhibition activity. Two different groups of quinazoline analogs were synthesized differ in the type of the 2-thioether function attached namely, 5-Amino-1,3,4-thiadiazole (**25**–**39**, **60**–**62**) as isosters to the lead compound **G** (IC_{50} 0.8 μM); and 2-amino-4-methylthiazole (**41**–**55**, **63**–**65**) as isosters to the lead compounds **H** and **I** (IC_{50} 0.5 and 0.3 μM, respectively). The 2-thioether function affects the magnitude of DHFR inhibition. The order of activity proved to be 5-Amino-1,3,4-thiadiazole (IC_{50} 0.4–1.0 μM) > 2-amino-4-methylthiazole (IC_{50} 1.0–2.0 μM). *In the 6-methyl series*, the presence of 3-phenyl and 2-(5-Amino-1,3,4-thiadiazol-2-yl-thio)-produced **25** with IC_{50} 7.0 μM with nine fold decrease in activity compared to **G**. Replacing of the 3-phenyl function of **25** by 3-benzyl group produced **60** with IC_{50} 2.0 μM with almost four folds increase in activity. The introduction of substituent at position 4- of the 3-phenyl function of **25** increased the activity producing the equipotent 3(4-chlorophenyl)-(**28**) with IC_{50} 0.7 μM and the eight fold more active analog 3(4-phenoxyphenyl)-**29** with IC_{50} 0.1 μM compared to **G**. The same analogy was also observed in the other *6-chloro* and *6,7-dimethoxy* series producing 2-(5-amino-1,3,4-thiadiazol-2-ylthio)-6-chloro-3-(4-phenoxyphenyl)-quinazolin-4(3*H*)-one (**34**), and 2-(5-amino-1,3,4-thiadiazol-2-ylthio)-6,7-dimethoxy-3-(4-phenoxy-phenyl)-quinazolin-4(3*H*)-one (**39**) with IC_{50} 0.4, 0.6 μM, respectively. In general, the type of substituent at positions 2-, 3-, and 6- of the quinazoline nucleus in addition to the 4-position of the 3-phenyl function proved to manipulate and contribute to the DHFR inhibition activity in the following order: 2-(5-Amino-1,3,4-thiadiazol-2-yl-thio)- > 2-(2-amino-4-methylthiazol-5-yl-thio)-; and 3-phenyl-> 3-benzyl-. The obtained antitumor results added another piece of evidence which empathize the order of activity what was concluded in the DHFR inhibition discussion that the 2-(5-Amino-1,3,4-thiadiazol-2-yl-thio)-series represented by compounds **26**, **33** and **39** is more active antitumors than the 2-(2-amino-4-methylthiazol-5-yl-thio)-series represented by compounds **43**, **44**, **50**, **55**, and **63**.

The DHFR inhibitory activity of the new synthesized compounds **25**–**39**, **41**–**55**, and **60**–**65** was experimentally determined. Compounds **29**, **34** and **39** proved to be the most active members in the present study (IC_{50} of 0.1, 0.4 and 0.6 μM, respectively) compared to the used positive control MTX (IC_{50}, 0.008 μM). Molecular modeling study was essentially needed to understand and interpret the unusual DHFR inhibitory pattern of this new class of compounds. It was interesting to start a comparative modeling study of the most active DHFR inhibitors **29**, **34** and **39** and the least active compounds **35** and **52** (IC_{50} of 10 and 8 μM, respectively) against MTX. The tertiary complex of human dihydrofolate reductase (hDHFR) crystal structure (pdb ID: 1DLS obtained from the protein data bank), NADPH and MTX were used as references for modeling and docking.[40–42] The binding of MTX to hDHFR is considered to be a complex interaction where hDHFR undergo some kind of

Table 3
Percentage growth inhibition (GI %) of in vitro subpanel tumor cell lines at 10 μM concentrations of compounds **26–39**

Subpanel tumor cell lines	% Growth inhibition[a,b] (GI %)								
	26	**30**	**32**	**33**	**34**	**35**	**37**	**38**	**39**
Leukemia									
CCRF-CEM	–	–	–	–	–	–	–	–	11.2
HL-60(TB)	28.2	21.5	–	–	12.0	–	–	31.5	22.5
K-562	–	–	–	–	–	–	–	15.3	29.6
MOLT-4	–	–	12.0	–	–	–	–	–	22.9
RPMI-8226	–	19.1	–	12.1	–	–	–	–	43.7
SR	32.7	–	19.1	–	–	–	–	14.4	57.3
Non-small cell lung cancer									
A549/ATCC	–	–	–	11.1	–	–	–	–	15.2
HOP-62	–	–	–	16.7	–	–	–	–	–
HOP-92	21.1	28.6	42.1	53.7	–	15.4	33.7	40.9	–
NCI-H226	–	–	13.4	–	–	–	–	–	13.4
NCI-H522	–	–	–	–	10.7	–	–	–	23.6
Colon cancer									
HCT-116	11.6	–	–	–	–	–	–	–	11.5
HCT-15	–	–	–	12.7	–	–	–	–	21.4
HT29	–	–	–	–	–	–	–	–	17.6
KM12	–	–	–	–	–	–	–	–	20.7
CNS cancer									
SF-295	–	–	11.0	20.6	–	10.6	–	12.1	–
SF-539	15.6	–	–	–	–	–	–	–	–
SNB-19	–	–	–	–	–	–	–	11.9	–
U251	–	–	–	11.0	–	–	–	11.5	–
Melanoma									
MALME-3 M	–	–	–	–	–	–	–	12.4	–
MDA-MB-435	–	–	–	10.8	–	–	–	–	–
SK-MEL-28	–	–	–	–	–	–	–	–	–
SK-MEL-5	–	–	–	10.9	–	–	–	–	28.2
UACC-257	–	–	–	12.3	–	–	–	–	–
UACC-62	14.8	–	–	–	–	–	–	–	22.1
Ovarian cancer									
OVCAR-4	–	–	–	–	–	–	–	–	34.6
Renal cancer									
786-0	–	–	–	15.4	–	–	–	–	–
A498	14.2	–	36.4	30.6	–	–	–	18.8	19.3
CAKI-1	10.4	–	–	–	–	–	–	12.6	–
RXF 393	10.5	–	–	–	–	–	–	–	10.7
UO-31	23.2	–	21.1	24.6	17.0	14.2	–	23.6	–
Prostate cancer									
PC-3	11.8	–	–	14.1	–	10.9	–	11.2	23.2
Breast cancer									
MCF7	–	16.4	13.2	12.7	–	–	–	–	14.8
MDA-MB-231/ATCC	21.9	–	–	–	–	–	–	–	–
BT-549	–	–	–	13.3	–	–	–	10.9	–
T-47D	–	21.4	12.0	29.2	–	–	–	13.7	38.4
MDA-MB-468	–	–	–	–	–	10.4	–	–	22.6

[a] GI < 10%; **nt**, not tested; **L**, compound proved lethal to the cancer cell line.
[b] Compounds **25**, **27–29**, **31**and **36** proved inactive.

isomerization or conformational change, resulting in tight binding, in addition to ionic bonding of N1 and 2-NH_2 to Glu30 (Fig. 1).[43–47] The calculated binding free energies were used as the parameter of selection for the cluster of docking posed to be evaluated in which the binding mode of the lowest energy structure located in the top docking cluster. The interaction of the most active derivative **29** with DHFR binding site shows key interaction with amino acid Glu30 in resemblance to MTX which explain the high inhibitory activity of this compound. Compound **34** binding mode revealed a triad interaction with DHFR binding site via arene–arene interaction with Phe31 and a side chain acceptor relationship with both carbonyl group of the quinazoline core and one of the nitrogens of the thiadiazole ring via ser59 and Try24, respectively. In case of **39** a tight binding interactions played a role in its DHFR inhibitory activity where a binary interaction of thiadiazole moiety bounded to Phe34 and to Glu30 which is in resemblance to MTX. The phenyl moiety of the quinazoline ring was embedded in a hydrophobic pocket constructed by the side chains of Tyr22 residue (Fig. 1). On the contrary, compound **35**, the least active derivative compared to **29**, lacks any interaction with the amino acids in the binding site of DHFR enzyme. In case of compound **52**, the only interaction occurred was between one of the methoxy groups and Arg77 residue which does not seem to have any impact on the biological activity (Fig. 2). To probe similarity between the 3D structures of the most active compound **29** and MTX, flexible alignment was employed. The initial approach was to employ MOE/MMFF94 flexible alignment to automatically generate superposition of the compounds under investigation with minimal user bias,[48] 200 conformers of each compound were generated and minimized with a distance-dependant dielectric model. A low energy set of 100 was selected for further analysis. The top scoring alignment with the least strain energy is shown in Figure 3. There

Table 4
Percentage growth inhibition (GI %) of in vitro subpanel tumor cell lines at 10 μM concentrations of compounds **43**–**55**, **60**–**64**

Subpanel tumor cell lines	% Growth inhibition[a,b] (GI %)										
	43	**44**	**46**	**48**	**50**	**51**	**55**	**61**	**62**	**63**	**64**
Leukemia											
CCRF-CEM	–	–	–	–	58.5	–	35.5	–	–	14.9	–
HL-60(TB)	–	–	–	–	40.6	–	21.2	24.3	–	–	–
K-562	13.0	15.6	–	14.3	25.7	–	21.5	24.8	–	17.4	17.6
MOLT-4	–	19.0	–	–	55.7	–	46.1	16.8	18.5	34.2	16.0
RPMI-8226	16.2	–	–	14.6	32.0	–	32.4	17.3	–	28.1	20.8
SR	–	49.2	–	13.5	L	15.0	L	–	13.4	19.0	16.1
Non-small cell lung cancer											
A549/ATCC	15.6	16.9	–	–	29.8	–	16.7	–	–	22.1	–
HOP-92	42.3	43.3	–	24.9	25.6	–	20.5	–	26.7	50.2	16.8
NCI-H226	–	–	–	11.8	13.6	–	10.3	–	–	22.7	10.4
NCI-H23	–	10.1	–	–	26.0	–	–	10.3	–	19.2	13.6
NCI-H460	–	–	–	–	18.0	–	–	–	–	–	–
NCI-H522	–	–	–	10.5	14.7	25.6	16.3	–	–	–	35.4
Colon cancer											
COLO 205	–	–	–	–	–	–	24.1	–	–	–	–
HCC-2998	–	–	–	–	26.0	–	19.6	–	–	–	–
HCT-116	19.1	22.8	–	–	66.7	–	52.7	–	–	20.7	–
HCT-15	25.3	27.7	–	–	44.6	–	20.1	–	–	13.5	–
HT29	–	11.7	–	–	44.1	–	25.0	–	–	–	–
KM12	19.4	24.6	–	–	20.2	–	–	–	–	18.8	–
SW-620	–	–	–	–	33.9	–	18.8	–	–	–	–
CNS cancer											
SF-268	10.6	13.2	–	–	–	–	–	–	–	10.8	13.3
SF-295	10.6	18.2	–	27.6	32.2	–	14.6	13.5	11.4	21.9	–
SF-539	–	13.9	–	–	–	–	18.7	–	–	15.1	–
SNB-19	15.5	11.6	–	–	30.7	–	–	–	–	–	–
SNB-75	11.9	–	–	–	–	–	13.3	–	–	22.7	–
U251	15.7	21.5	–	–	22.8	–	12.4	–	–	12.2	–
Melanoma											
LOX IMVI	11.0	16.5	–	–	24.5	–	21.7	–	–	19.5	23.2
MALME-3M	–	–	–	–	–	–	–	19.2	–	–	15.9
M14	–	15.6	–	–	23.4	–	18.5	–	–	10.3	–
MDA-MB-435	–	–	–	–	11.9	–	–	–	–	–	–
SK-MEL-5	15.7	16.3	–	–	23.9	–	23.2	–	–	25.8	–
UACC-257	–	13.6	–	–	24.3	–	10.3	–	–	11.6	–
UACC-62	15.4	26.0	–	12.6	36.1	–	18.6	17.5	–	22.8	15.2
Ovarian cancer											
OVCAR-3	–	–	–	–	–	–	–	–	–	19.2	14.9
OVCAR-4	12.9	–	–	13.8	59.1	–	49.3	–	–	18.7	20.9
OVCAR-5	17.9	12.1	–	–	12.1	–	–	–	–	–	–
OVCAR-8	13.4	10.8	–	–	24.9	–	15.0	–	–	16.0	–
NCI/ADR-RES	11.3	17.5	–	–	30.1	–	24.8	–	–	20.3	–
Renal cancer											
786-0	12.0	29.3	–	–	31.5	–	20.0	–	–	–	–
A498	24.6	53.0	–	24.3	60.2	–	18.0	25.9	18.7	21.9	–
ACHN	–	–	–	–	21.5	–	18.5	–	–	19.8	–
CAKI-1	11.5	11.2	–	13.1	26.5	–	–	–	–	13.7	–
RXF 393	28.0	28.5	–	13.4	13.4	–	14.1	–	–	17.8	–
SN12C	–	12.8	–	–	26.1	–	20.3	–	–	–	–
TK-10	–	–	–	–	11.1	–	–	–	–	–	–
UO-31	26.2	46.0	32.6	35.5	38.3	32.3	23.9	27.2	21.5	35.5	36.4
Prostate cancer											
PC-3	15.9	28.6	–	14.7	51.1	–	34.9	12.8	–	34.5	15.8
Breast cancer											
MCF7	–	–	18.0	11.5	12.6	21.7	25.7	–	–	10.7	–
MDA-MB-231/ATCC	25.0	13.0	–	–	10.7	–	–	–	–	14.2	–
HS 578T	–	12.6	–	–	18.1	–	11.6	–	–	19.4	–
BT-549	20.6	33.1	–	–	36.8	–	28.7	–	–	–	–
T-47D	–	12.4	14.3	–	24.5	–	22.7	–	–	23.9	14.7
MDA-MB-468	–	–	–	–	23.4	–	19.9	–	–	30.1	–

[a] GI < 10%; **nt**, not tested; **L**, compound proved lethal to the cancer cell line.
[b] Compounds **41**, **42**, **45**, **47**, **49**, **52**–**54**, **60** and **65** proved inactive.

is a good alignment between MTX and **29** explaining their resemblance in binding mode flipped profile into DHFR binding site. Compound **29** (the most active compound) was chosen as the template molecule, on which other molecules were aligned. Thirteen low energy, maximally dissimilar structures were selected for comparison to the other compounds. After assigning MMFF94 charges to all molecules, flexible alignment was ranked by overlays of compounds **29**, **34** and **39** based on electrostatic, steric field, hydrophobic areas overlap, hydrogen bond acceptors and donors overlap. From the highest scoring superposition, the limited set

Please cite this article in press as: Al-Rashood, S. T.; et al. *Bioorg. Med. Chem. Lett.* (2014), http://dx.doi.org/10.1016/j.bmcl.2014.07.070

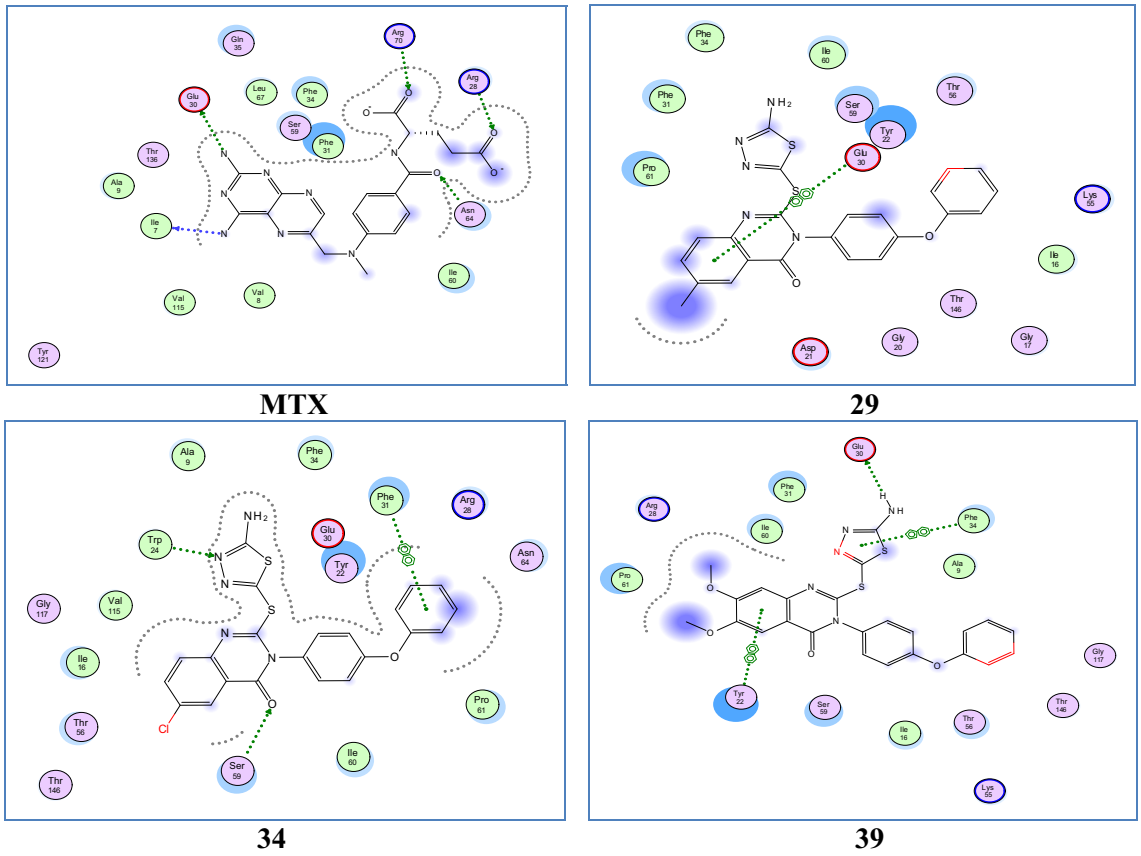

Figure 1. The 2D binding mode and residues involved in the recognition for MTX, the most active compounds **29** (IC_{50} 0.1 μM), **34** (IC_{50} 0.4 μM) and **39** (IC_{50} 0.6 μM) docked and minimized in the DHFR binding pocket. The essential amino acid residues at the binding site are tagged in circles.

of conformers was used in the analysis of molecules with high flexibility capable to achieving complete atom to atom superposition. A common feature of the MOE-generated alignments was that the three structures showed matched quinazoline and phenoxy rings, and slight differences in the distance the between methyl and thiadiazole moieties (0.16 Å, Fig. 4a). Adopting the same methodology, the most active DHFR inhibitors **29**, **34**, **39** and the least active compounds **35** and **52** were subjected to flexible alignment analysis (Fig. 4b). It is an important experiment to gain a clear vision of the essential features for a given activity. It is clear that compounds **35** and **52** were flexibly aligned in a different manner when compared with the active compound **29**. Common feature of the MOE-generated alignments showed that the super position is occurred among the compounds where a deviation distance of about 2.23 Å compared with the least active compounds. These features explain the difference in activity among the two groups and show the importance of the phenoxy moiety attached to quinazoline N atom. An attempt to investigate the reasons behind the diminished DHFR inhibition activity of compound **35**, electrostatic mapping was carried out for its lowest energy conformer to study the similarity and dissimilarity of the electrostatic binding characteristics of the molecule surface and its conformational properties, in comparison to the most active compound **29**. Figure 5a showed some common features of **29**, having more

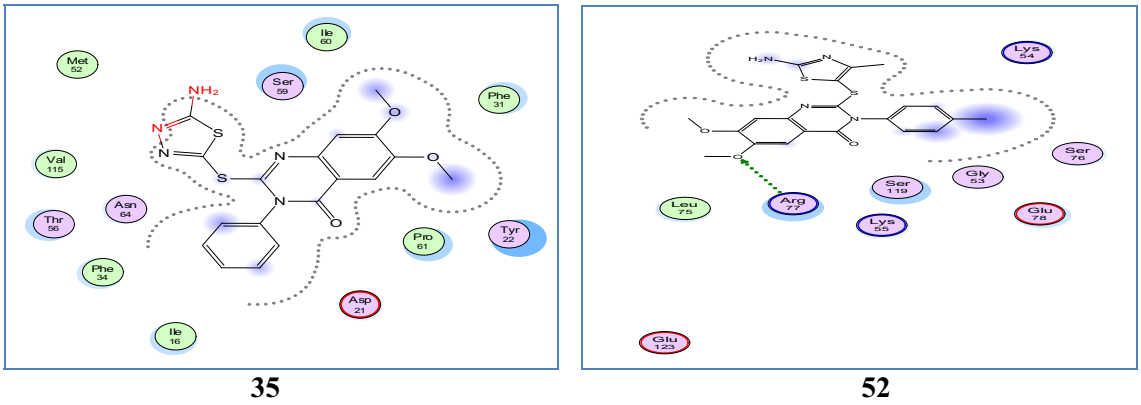

Figure 2. The 2D binding mode and residues involved in the recognition for the inactive compounds **35** (IC_{50} 10.0 μM) and **52** (IC_{50} 8.0 μM) docked and minimized in the DHFR binding pocket. The essential amino acid residues at the binding site are tagged in circles.

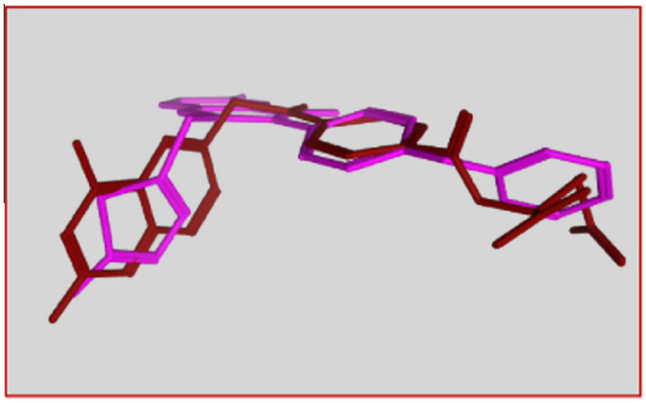

Figure 3. Flexible alignment of the most active compound **29** (pink) and MTX (brown).

hydrophobic regions distributed all over the molecule, on the contrary the least active DHFR inhibitor which showed scattered mild Polar Regions (Fig. 5b). The obtained hydrophobic mapping conformations suggest a distinct varied interaction of the active and inactive molecules with the potential protein binding site. Oral bioavailability plays an important role in the development of bioactive molecules into therapeutic agents. Many potential therapeutic agents fail to reach the clinic because of their unfavorable absorption, distribution, metabolism, elimination and toxic (ADMET) factors.[49] Therefore, a computational study for the prediction of ADMET properties of compounds **29**, **34** and **39** was performed for the determination of topological polar surface area (TPSA), and the 'rule of five' formulated by Lipinski[50] for the activity prediction of an orally administered drug, if it has no more than one violation of the following rules: (i) *C*log*P* (partition coefficient between water and octanol) <5; (ii) number of hydrogen bond donors sites ⩽5; (iii) number of hydrogen bond acceptor sites ⩽10; (iv), molecular weight <500; (v) No. of rotatable bonds <5. In addition, the total polar surface area (TPSA) is another key property linked to drug bioavailability; the passively absorbed molecules with TPSA >140 have low oral bioavailability.[51] All calculated descriptors were obtained using the MOE package, and the results are listed in Table 5. The obtained results revealed that the *C*Log*P* are around 5.0 for compounds **29** and **39** and less than 5.0 for compound **34**, the molecular weight was less than 500, except for compound **39** (505.57), hydrogen bond acceptor <10 and hydrogen bond donors <5 which fulfill Lipinski's rule. Also, the percent absorption of compounds **39** total surface area with 253.31 shows the lowest bioavailability among all tested compounds. From these data, it could be suggested that compounds

Table 5
Pharmacokinetic parameters of compounds **29**, **34** and **39**

Compd	Mwt	TPSA	Log*P*	Lip. don	Lip. acc	Lip. V	b.rotN
29	459.55	94.95	5.06	2	7	5.66	5
34	479.94	96.14	4.35	2	7	6.00	5
39	505.57	253.31	5.46	2	9	5.37	7

TPSA: Polar surface area, Log*P*: Calculated lipophilicity, Lip.don: Number of hydrogen bond donors, Lip.acc: Number of hydrogen bond acceptors, Lip.V: Number of violations of Lipinski rule, b.rotN: No. of rotatable bonds.

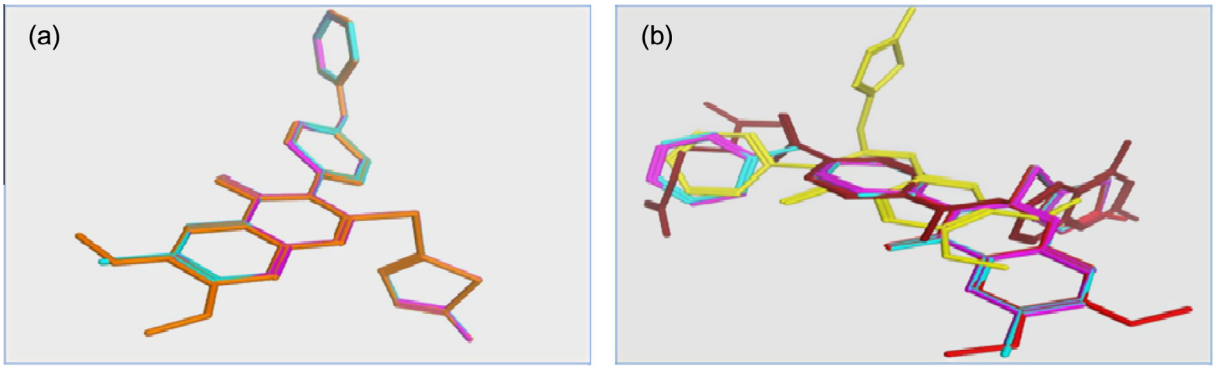

Figure 4. (a) Flexible alignment of the most active compounds **29** (pink), **34** (cyan) and **39** (orange). (b) Flexible alignment of the most active compounds **29** (pink), **34** (cyan) and **39** (orange) against inactive compounds **35** (yellow) and **52** (brown).

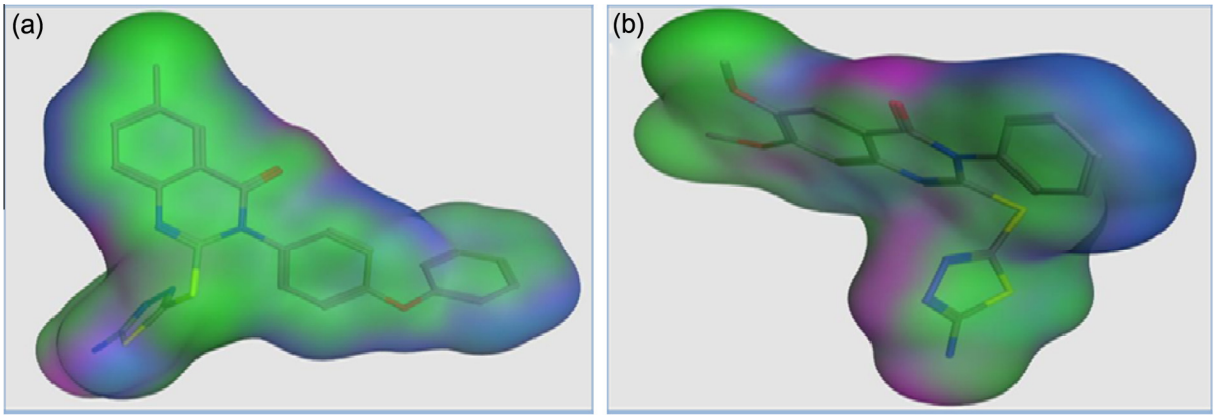

Figure 5. Surface map for (a) the most active compound **29**; (b) the least active compound **35**. Pink: hydrogen bond, blue: mild polar, green: hydrophobic region.

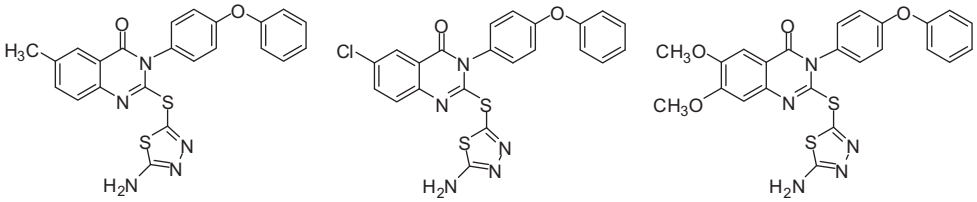

Figure 6. Structures of the active DHFR inhibitors **29**, **34** and **39**.

29 and **34** can be used as good orally absorbed anticancer agents with diminished toxicity among the investigated compounds.

In conclusion, compounds **29**, **34** and **39** (Fig. 6) proved to be the most active DHFR inhibitors with IC_{50} values range of 0.1–0.6 μM. Structure activity relationship studies revealed that, in general, the type of substituent at positions 2-, 3-, and 6- of the quinazoline nucleus proved to manipulate and contribute to the DHFR inhibition activity in the following order: 2-(5-Amino-1,3,4-thiadiazol-2-yl-thio)- > 2-(2-amino-4-methylthiazol-5-yl-thio)-; and 3-phenyl- > 3-benzyl-. Compounds **28**, **31** and **33** showed a remarkable broad-spectrum activity against both Gram-positive and Gram-negative bacteria. Compounds **28** and **33** might exert their activity through DHFR inhibition. Meanwhile, compounds **26**, **33**, **39**, **43**, **44**, **50**, **55** and **63** showed broad spectrum potency toward several tumor cell lines with GI values range of 10.1–100%. Compounds **33**, **39** and **50** might exert their antitumor activity through DHFR inhibition. Molecular modeling study was performed and concluded that recognition with key amino acid Glu30, Phe31 and Phe34 is essential for binding and biological activities of the investigated quinazolines. Computational study for the prediction of ADMET properties of the active compounds suggested that compounds **29** and **34** could be used as orally absorbed agents with diminished toxicity. Therefore, the obtained model could be used as useful template for the development of new DHFR inhibitors.

Acknowledgments

The authors express their appreciation and thanks to the 'Research Center of the Female Scientific and Medical Colleges', Deanship of Scientific Research, King Saud University, for their valuable Grant.

Supplementary data

Supplementary data associated with this article can be found, in the online version, at http://dx.doi.org/10.1016/j.bmcl.2014.07.070.

References and notes

1. Masur, H. *J. Infect. Dis.* **1990**, *161*, 858.
2. Berman, E. M.; Werbel, L. M. *J. Med. Chem.* **1991**, *34*, 479.
3. Borst, P.; Quellette, M. *Annu. Rev. Microbiol.* **1995**, *49*, 427.
4. Green, E.; Demos, C. H. In *Folate Antagonists as Therapeutic Agents*; Sirotank, F. M., Burchall, J. J., Ensminger, W. B., Montgomery, J. A., Eds.; ; Academic Press: Orlando, 1984; Vol. 2, p 191.
5. Mullarkey, M. F.; Blumenstein, B. A.; Andrade, W. P.; Bailey, G. A.; Olason, I.; Weizel, C. E. *Engl. J. Med.* **1988**, *318*, 603.
6. Elslager, E. F.; Elslager, J.; Johnson, L.; Werbel, L. M. *J. Med. Chem.* **1983**, *26*, 1753.
7. Grivsky, E. M.; Lee, S.; Sigel, C. W.; Duch, D. S.; Nichol, C. A. *J. Med. Chem.* **1980**, *23*, 327.
8. Bavetsias, V.; Jackman, A. L.; Marriott, J. H.; Kimbell, R.; Gibson, W.; Boyle, F. T.; Bisset, G. M. *J. Med. Chem.* **1997**, *40*, 1495.
9. Bavetsias, V.; Marriott, J. H.; Melin, C.; Kimbell, R.; Matusiak, Z. S.; Boyle, F. T.; Jackman, A. L. *J. Med. Chem.* **2000**, *43*, 1910.
10. Werbel, L. M.; Degnan, M. J. *J. Med. Chem.* **1987**, *30*, 2151.
11. Sheng-Li, C.; Yu-Ping, F.; Yu-Yang, J.; Shi-Ying, L.; Guo-Yu, D.; Run-tao, L. *Bioorg. Med. Chem. Lett.* **2005**, *15*, 1915.
12. Wyss, P. C.; Gerber, P.; Hartman, P. G.; Hubschwerlen, C.; Locher, H.; Marty, H.; Stahl, M. *J. Med. Chem.* **2003**, *46*, 2304.
13. Al-Rashood, S. T.; Aboldahab, I. A.; Abouzeid, L. A.; Abdel-Aziz, A. A.-M.; Nagi, M. N.; Abdulhamide, S. G.; Youssef, K. M.; Al-Obaid, A. M.; El-Subbagh, H. I. *Bioorg. Med. Chem.* **2006**, *14*, 8608.
14. Al-Omary, F. A. M.; Abou-zeid, L. A.; Nagi, M. N.; Habib, E. E.; Abdel-Aziz, A. A.-M.; El-Azab, A. S.; Abdel-Hamide, S. G.; Al-Omar, M. A.; Al-Obaid, A. M.; El-Subbagh, H. I. *Bioorg. Med. Chem.* **2010**, *18*, 2849.
15. Al-Omary, F. A. M.; Hassan, G. S.; El-Messery, S. M.; Nagi, M. N.; Habib, E. E.; El-Subbagh, H. I. *Eur. J. Med. Chem.* **2013**, *63*, 33.
16. Hassan, G. S.; El-Messery, S. M.; Al-Omary, F. A. M.; Al-Rashood, S. T.; Shabayek, M. I.; Abulfadl, Y. S.; Habib, E. E.; El-Hallouty, S. M.; Fayad, W.; Mohamed, K. M.; El-Menshawi, B. S.; El-Subbagh, H. I. *Eur. J. Med. Chem.* **2013**, *66*, 135.
17. El-Subbagh, H. I.; Hassan, G. S.; El-Messery, S. M.; Al-Omary, F. A. M.; Al-Rashood, S. T.; Abulfadl, Y. S.; Shabayek, M. I. *Eur. J. Med. Chem.* **2014**, *74*, 234.
18. El-Subbagh, H. I.; El-Sherbeny, M. A.; Nasr, M. N.; Goda, F. E.; Badria, F. A. *Boll. Chim. Farmaceutico* **1995**, *134*, 80.
19. El-Subbagh, H. I.; Abadi, A. H.; Al-Khamees, H. A. *Arch. Pharm. Pharm. Med. Chem.* **1997**, *330*, 277.
20. El-Obaid, A. M.; El-Shafie, F. S.; Al-Mutairi, M. S.; El-Subbagh, H. I. *Sci. Pharm.* **1999**, *67*, 129.
21. El-Subbagh, H. I.; Abadi, A. H.; El-Khawad, I. E.; Rashood, K. A. *Arch. Pharm. Pharm. Med. Chem.* **1999**, *332*, 19.
22. Al-Obaid, A. M.; El-Subbagh, H. I.; Khodair, A. I.; El-mazar, M. M. *Anticancer Drugs* **1996**, *7*, 873.
23. El-Subbagh, H. I.; Abu-Zaid, S. M.; Mahran, M. A.; Badria, F. A.; Al-Obaid, A. M. *J. Med. Chem.* **2000**, *43*, 2915.
24. Al-Madi, S. H.; Al-Obaid, A. M.; El-Subbagh, H. I. *Anticancer Drugs* **2001**, *12*, 835.
25. Abdel Hamid, S. G.; El-Obaid, H. A.; Al-Rashood, K. A.; Khalil, A. A.; El-Subbagh, H. I. *Sci. Pharm.* **2001**, *69*, 351.
26. Khalil, A. A.; Abdel Hamide, S. G.; Al-Obaid, A. M.; El-Subbagh, H. I. *Arch. Pharm. Pharm. Med. Chem.* **2003**, *336*, 95.
27. El-Subbagh, H. I.; Al-Obaid, A. M. *Eur. J. Med. Chem.* **1996**, *31*, 1017.
28. El-Subbagh, H. I.; El-Naggar, W. A.; Badria, F. A. *Med. Chem. Res.* **1994**, *3*, 503.
29. Abdel Hamid, S. G.; El-Obaid, H. A.; Al-Majed, A. A.; El-Kashef, H. A.; El-Subbagh, H. I. *Med. Chem. Res.* **2001**, *10*, 378.
30. Al-Omar, M. A.; AbdelHamide, S. G.; Al-Khamees, H. A.; El-Subbagh, H. I. *Saudi Pharm. J.* **2004**, *12*, 63.
31. Foye, W. O.; Lemke, T. L.; Williams, D. A. *Principles of Medicinal Chemistry*, 4th Ed.; Williams and Wilkins: Media, PA, 2005. p 442.
32. Nordberg, M. G.; Kolmodin, K.; Aqvist, J.; Queener, S. F.; Hallberg, A. *J. Med. Chem.* **2001**, *44*, 2391.
33. Grever, M. R.; Schepartz, S. A.; Chabner, B. A. *Semin. Oncol.* **1992**, *19*, 622.
34. Monks, A.; Scudiero, D.; Skehan, P. *J. Natl. Cancer Inst.* **1991**, *83*, 757.
35. Boyd, M. R.; Paull, K. D. *Drug Rev. Res.* **1995**, *34*, 91.
36. Skehan, P.; Storeng, R.; Scudiero, D.; Monks, A.; McMahon, J.; Vistica, D.; Warren, J. R.; Bokesch, H.; Kenney, S.; Boyd, M. R. *J. Natl. Cancer Inst.* **1990**, *82*, 1107.
37. Pignatello, R.; Sapmpinato, G.; Sorrenti, V.; Vicari, L.; Di-Giacomo, C.; Vanella, A.; Puglisi, G. *Pharm. Pharmacol. Commun.* **1999**, *5*, 299.
38. Clinical and Laboratory Standards Institute (CLSI). Performance standards for antimicrobial susceptibility testing, CLSI approved standards M100–S15., Wayne, PA, 2008.
39. Murray, P. R.; Baron, E. J.; Pfaller, M. A.; Tenover, F. C.; Yolken, R. H. In *Manual of Clinical Microbiology*; Wood, G. L., Washington, J. A., Eds.; Am. Soc. Microbiol.: Washington D.C., 1995.
40. Gokhale, V. M.; Kulkarni, V. M. *J. Comput. Aided Mol. Des.* **2000**, *14*, 495.
41. Klon, A. E.; Heroux, A.; Ross, L. J.; Pathak, V.; Johnson, C. A.; Piper, J. R.; Borhani, D. W. *J. Mol. Biol.* **2002**, *320*, 677.
42. Al-Obaid, A. M.; Abdel-Hamide, S. G.; El-Kashef, H. A.; Abdel-Aziz, A. A.-M.; El-Azab, A. S.; Al-Khamees, H. A.; El-Subbagh, H. I. *Eur. J. Med. Chem.* **2009**, *44*, 2379.
43. Appleman, J. R.; Beard, W. A.; Delcamp, T. J.; Prendergast, N. J.; Freisheim, J. H.; Blakley, R. L. *J. Biol. Chem.* **1988**, *263*, 10304.
44. Blakley, R. L.; Cocco, L. *Biochemistry* **1985**, *24*, 4772.

45. Davies, J. F.; Delcamp, T. J.; Prendergast, N. J.; Ashford, V. A.; Freisheim, J. H.; Kraut, J. *Biochemistry* **1990**, *29*, 9467.
46. Oefner, C.; D'Arcy, A.; Winkle, F. K. *Eur. J. Biochem.* **1988**, *174*, 377.
47. Stockman, B. J.; Nirmala, N. R.; Wagner, G.; Delcamp, T. J.; DeYarman, M. T.; Freisheim, J. H. *FEBS Lett.* **1991**, *283*, 267.
48. Kearsley, S.; Smith, G. M. *Tetrahedron Comput. Methodol.* **1990**, *3*, 615.
49. Zhao, Y.; Abraham, M. H.; Lee, J.; Hersey, A.; Luscombe, N. C.; Beck, G.; Sherborne, B.; Cooper, I. *Pharm. Res.* **2002**, *19*, 1446.
50. Lipinski, C. A.; Lombardo, F.; Dominy, B. W.; Feeney, P. J. *Adv. Drug. Delivery Rev.* **1997**, *23*, 3.
51. Clark, D. E.; Pickett, S. D. *Drug Discov. Today* **2000**, *5*, 49.

Please cite this article in press as: Al-Rashood, S. T.; et al. *Bioorg. Med. Chem. Lett.* (2014), http://dx.doi.org/10.1016/j.bmcl.2014.07.070